

Controlled Stoichiometry for Quaternary CuIn_xGa_{1-x}S₂ Chalcopyrite Nanoparticles from Single-Source Precursors via Microwave Irradiation

Chivin Sun,[†] Joseph S. Gardner,[‡] Gary Long,[†] Cyril Bajracharya,[†] Aaron Thurber,[§] Alex Punnoose,[§] Rene G. Rodriguez,^{*,†} and Joshua J. Pak^{*,†}

[†]Department of Chemistry, Idaho State University, Pocatello, Idaho 83209, [‡]Department of Physical Science, College of Southern Idaho, Twin Falls, Idaho 83303, and [§]Department of Physics, Boise State University, Boise, Idaho 83725

Received February 12, 2010
Revised Manuscript Received April 7, 2010

In recent years, there have been several reports on the formation of I–III–VI₂ nanoparticles through the decomposition of single-source precursors (SSPs) using thermolysis,^{1–7} photolysis,⁸ and microwave irradiation.^{9,10} Uses of SSPs in preparation of nanomaterials present distinct advantages such as precise control in reaction conditions and stoichiometry as SSPs contain all necessary elements in a single molecule. Despite the obvious advantages of SSPs, to the best of our knowledge, no studies have been conducted using combinations of SSPs to form quaternary or multinary chalcopyrite nanoparticles.

Previously, we reported the size-controlled preparation of CuInS₂ nanoparticles from SSP, (Ph₃P)₂Cu(μ-SEt)₂In(SET)₂ (**1**), via microwave irradiation.¹⁰ As we looked to expand our method to prepare quaternary nanoparticles, we discovered that mixing of two SSPs containing In and Ga can provide desired products without sacrificing stoichiometric control in resulting nanoparticles. In recent years, there have been a limited number of reports describing the preparation of related multinary nanoparticles from multiple sources. For example, Nakamura et al., successfully

prepared Zn–Cu–In–Ga–S (Zn:Cu:In:Ga:S = 1:*n*:*n*:4, where *n* = 0.5–4).¹¹ Pan et al. recently reported the synthesis of quaternary Cu_{1.0}Ga_{*x*}In_{2-*x*}S_{3.5} (0 ≤ *x* ≤ 2) nanocrystals with tunable bandgaps by increasing the indium content.¹² In addition, there have been some exciting reports of incorporating similar nanoparticles into photovoltaic devices with promising results.^{13–17}

In our studies, we prefer microwave-assisted growth of nanoparticles over traditional thermolysis as microwave provides greater homogeneity in the overall reaction temperature.¹⁸ This allows for the preparation of nanoparticles with diameters of a few nanometers,¹⁹ dramatic decreases in reaction times, improved product purities, the use of many forms of precursors, and reactions exhibiting good reproducibility and high yields.^{10,20}

Herein, we report efficient syntheses of the quaternary CuIn_{*x*}Ga_{1-*x*}S₂ (0 ≤ *x* ≤ 1) chalcopyrite nanoparticles with precise stoichiometric control by decomposition of a mixture of two I–III bimetallic SSPs in the presence of 1,2-ethanedithiol via microwave irradiation.

In a typical reaction, a combination of two SSPs, (Ph₃P)₂Cu(μ-SEt)₂In(SET)₂ (**1**) and (Ph₃P)₂Cu(μ-SEt)₂Ga(SET)₂ (**2**),^{3,21,22} are dissolved in benzyl acetate in the presence of 1,2-ethanedithiol and irradiated with microwave and held at a desired reaction temperature for less than 1 h. Resulting nanoparticles exhibit darker colors as a function of increasing In content and represent respective bandgap changes in CuIn_{*x*}Ga_{1-*x*}S₂ nanoparticles as shown in Figure 1. The qualitative comparison of the XPS data indicates that we can indeed prepare nanoparticles which contain Cu, In, Ga, and S as well as carbon from the 1,2-ethanedithiol (see the Supporting Information). The modulation between Ga and In in the quaternary nanoparticles is clearly reflected in the XPS data (see the Supporting Information). When SSP **1** was mixed with

*Corresponding author. E-mail: rodrrene@isu.edu (R.G.R.); pakjosh@isu.edu (J.J.P.).

- (1) Castro, S. L.; Bailey, S. G.; Raffaele, R. P.; Banger, K. K.; Hepp, A. F. *J. Phys. Chem. B* 2004, 108, 12429–12435.
- (2) Castro, S. L.; Bailey, S. G.; Raffaele, R. P.; Banger, K. K.; Hepp, A. F. *Chem. Mater.* 2003, 15, 3142–3147.
- (3) Banger, K. K.; Jin, M. H. C.; Harris, J. D.; Fanwick, P. E.; Hepp, A. F. *Inorg. Chem.* 2003, 42, 7713–7715.
- (4) Han, S.; Kong, M.; Guo, Y.; Wang, M. *Mater. Lett.* 2009, 63, 1192–1194.
- (5) Zhong, H.; Zhou, Y.; Ye, M.; He, Y.; Ye, J.; He, C.; Yang, C.; Li, Y. *Chem. Mater.* 2008, 20, 6434–6443.
- (6) Dutta, D. P.; Sharma, G. *Mater. Lett.* 2006, 60, 2395–2398.
- (7) Deivaraj, T. C.; Park, J. H.; Afzaal, M.; O'Brien, P.; Vittal, J. J. *Chem. Mater.* 2003, 15, 2383–2391.
- (8) Nairn, J. J.; Shapiro, P. J.; Twamley, B.; Pounds, T.; von Wandruszka, R.; Fletcher, T. R.; Williams, M.; Wang, C.; Norton, M. G. *Nano Lett.* 2006, 6, 1218–1223.
- (9) Gardner, J. S.; Shurdha, E.; Wang, C.; Lau, L. D.; Rodriguez, R. G.; Pak, J. J. *J. Nanopart. Res.* 2008, 10, 633–641.
- (10) Sun, C.; Gardner, J. S.; Shurdha, E.; Margulieux, K. R.; Westover, R. D.; Lau, L.; Long, G.; Bajracharya, C.; Wang, C.; Thurber, A.; Punnoose, A.; Rodriguez, R. G.; Pak, J. J. *J. Nanomater.* 2009, 2009, 748567.

- (11) Nakamura, H.; Kato, W.; Uehara, M.; Nose, K.; Omata, T.; Otsuka-Yao-Matsuo, S.; Miyazaki, M.; Maeda, H. *Chem. Mater.* 2006, 18, 3330–3335.
- (12) Pan, D.; Wang, X.; Hong Zhou, Z.; Chen, W.; Xu, C.; Lu, Y. *Chem. Mater.* 2009, 21, 2489–2493.
- (13) Tang, J.; Hinds, S.; Kelley, S. O.; Sargent, E. H. *Chem. Mater.* 2008, 20, 6906–6910.
- (14) Panthani, M. G.; Akhavan, V.; Goodfellow, B.; Schmidtke, J. P.; Dunn, L.; Dodabalapur, A.; Barbara, P. F.; Korgel, B. A. *J. Am. Chem. Soc.* 2008, 130, 16770–16777.
- (15) Merdes, S.; Sáez-Araoz, R.; Ennaoui, A.; Klaer, J.; Lux-Steiner, M. Ch.; Klenk, R. *Appl. Phys. Lett.* 2009, 95, 213502–213504.
- (16) Guo, Q.; Ford, G. M.; Hillhouse, H. W.; Agrawal, R. *Nano Lett.* 2009, 9, 3060–3065.
- (17) Yuan, M.; Mitzi, D. B.; Liu, W.; Kellock, A. J.; Chey, S. J.; Deline, V. R. *Chem. Mater.* 2010, 22, 285–287.
- (18) Gerbec, J. A.; Magana, D.; Washington, A.; Strouse, G. F. *J. Am. Chem. Soc.* 2005, 127, 15791–15800.
- (19) Zhu, J.; Plachik, O.; Chen, S.; Gedanken, A. J. *J. Phys. Chem. B* 2000, 104, 7344–7347.
- (20) Grisaru, H.; Palchik, O.; Gedanken, A. *Inorg. Chem.* 2003, 42, 7148–7155.
- (21) Hirpo, W.; Dhingra, S.; Sutorik, A. C.; Kanatzidis, M. G. *J. Am. Chem. Soc.* 1993, 115, 1597–1599.
- (22) Margulieux, K. R.; Sun, C.; Zakharov, L. N.; Holland, A. W.; Pak, J. J. *Inorg. Chem.* 2010, ASAP.

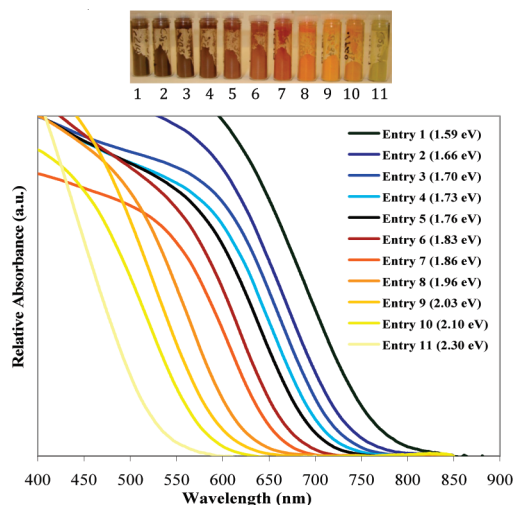


Figure 1. Normalized UV-vis absorption spectra of $\text{CuIn}_x\text{Ga}_{1-x}\text{S}_2$ nanoparticles prepared at 160 °C with bandgaps.

Table 1. Composition (from ICP-OES analysis) and Optical Bandgaps (E_g) (from UV-vis spectra) of $\text{CuIn}_x\text{Ga}_{1-x}\text{S}_2$ Nanoparticles Prepared at 160 °C

entry	SSP 1/2	Cu % ^a	In % ^a	Ga % ^a	In+Ga	E_g (eV)
1	1.0/0.0	18.48	17.64	0.00	17.64	1.59
2	0.9/0.1	19.67	17.49	2.16	19.65	1.66
3	0.8/0.2	20.14	16.09	3.81	19.90	1.70
4	0.7/0.3	20.23	14.45	5.81	20.26	1.73
5	0.6/0.4	20.48	12.89	7.49	20.38	1.76
6	0.5/0.5	20.50	10.62	9.59	20.21	1.83
7	0.4/0.6	20.74	8.85	12.00	20.85	1.86
8	0.3/0.7	20.93	6.88	13.58	20.46	1.96
9	0.2/0.8	21.23	4.96	15.63	20.59	2.03
10	0.1/0.9	21.85	3.31	17.80	21.11	2.10
11	0.0/1.0	21.36	0.00	19.01	19.01	2.30

^aThe measurements by ICP-OES have an error of ± 0.2 atom % for Cu, ± 0.5 atom % for In, and ± 0.2 atom % for Ga.

increasing amounts of SSP 2 under the reaction conditions, the resulting nanoparticles contained increasing amounts of Ga as expected (Table 1).

The analysis of $\text{CuIn}_x\text{Ga}_{1-x}\text{S}_2$ nanoparticles by ICP-OES (Table 1) indicates that our method allows precise control of In and Ga. The high level of control is most likely due to the fact that 1,2-ethanedithiol acts as a bridging unit between two SSP units.¹⁰ This process produces cross-linked random polymers of SSPs, which undergo rapid decomposition to produce the resulting $\text{CuIn}_x\text{Ga}_{1-x}\text{S}_2$ nanoparticles.¹⁰ This is supported by the fact that replacing 1,2-ethanedithiol with 1-hexanedithiol resulted in poor metal ratio control (see the Supporting Information).

As shown in Figure 1, the absorption peak shifts to lower energy when the nanoparticles are grown at higher concentrations of In. The bandgap range (1.59–2.30 eV) achieved by our $\text{CuIn}_x\text{Ga}_{1-x}\text{S}_2$ ($0 \leq x \leq 1$) nanoparticles fits nicely between the bandgaps of the bulk CuInS_2 (1.50 eV) and CuGaS_2 (2.40 eV).

The estimated volume-weighted crystal diameters (Scherrer equation with a shape factor of 0.9)²³ of our

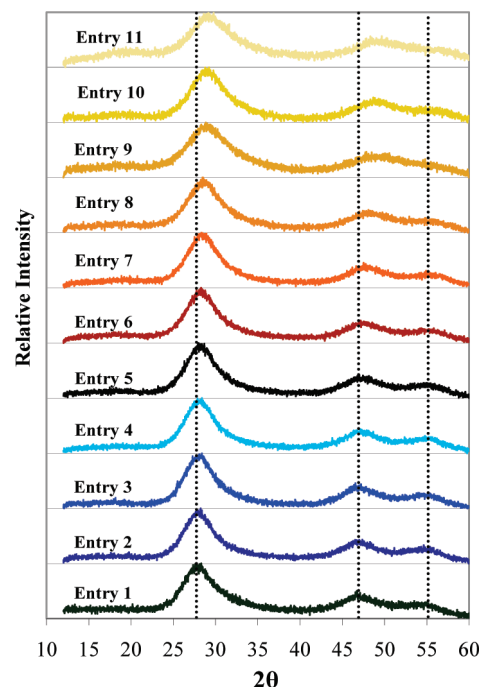


Figure 2. Normalized XRD data of $\text{CuIn}_x\text{Ga}_{1-x}\text{S}_2$ nanoparticles prepared at 160 °C.

Table 2. Composition, Sizes, and Optical Bandgaps (E_g) of $\text{CuIn}_{0.5}\text{Ga}_{0.5}\text{S}_2$ Nanoparticles Prepared from 160–240 °C

entry	T (°C)	Cu % ^a	In % ^a	Ga % ^a	size (nm)	E_g (eV)
12	160	20.50	10.62	9.59	2.9	1.83
13	180	20.95	9.77	9.74	3.2	1.80
14	200	21.82	10.16	10.26	3.4	1.76
15	220	22.59	9.72	10.79	3.7	1.71
16	240	22.66	10.99	10.72	4.3	1.64

^aThe measurements by ICP-OES have an error of ± 0.2 atom % for Cu, ± 0.5 atom % for In, and ± 0.2 atom % for Ga.

samples range from 2.7 to 3.3 nm as a function of increasing In content (Figure 2). The XRD patterns show three major peaks at $2\theta = 28.0, 46.4,$ and 55.0° for CuInS_2 , and at $2\theta = 29.1, 48.7,$ and 57.2° for CuGaS_2 . The peaks are consistent with chalcopyrite for CuInS_2 reference pattern 85–1575 (JCPDS-03–065–2732) and CuGaS_2 reference pattern 25–0279 (JCPDS-01–082–1531). These quaternary nanoparticles are most likely chalcopyrite phase with major peaks shifting toward narrower lattice spacing as expected, as a function of increasing Ga content.^{14,16}

To determine the effects of the reaction temperature in the In:Ga ratio, we irradiated the 1:1 mixture of SSPs 1 and 2 via microwave from 160 to 240 °C under the analogous condition. According to the ICP-OES data (Table 2), the resulting nanoparticles are slightly Cu-rich and In:Ga ratios were approximately 1:1 at various temperatures. In addition, larger nanoparticles were formed as a function of increasing reaction temperatures as indicated by decreasing bandgaps ranging from 1.83 to 1.64 eV (Figure 3). At 240 °C, quaternary $\text{CuIn}_x\text{Ga}_{1-x}\text{S}_2$ ($0 \leq x \leq 1$) chalcopyrite nanoparticles were also successfully synthesized with bandgap ranging from 1.90 to 1.40 eV and size ranging from 3.7 to 5.9 nm (see the Supporting Information).

(23) Natter, H.; Schmelzer, M.; Löffler, M. S.; Krill, C. E.; Fitch, A.; Hempelmann, R. *J. Phys. Chem. B* **2000**, *104*, 2467–2476.

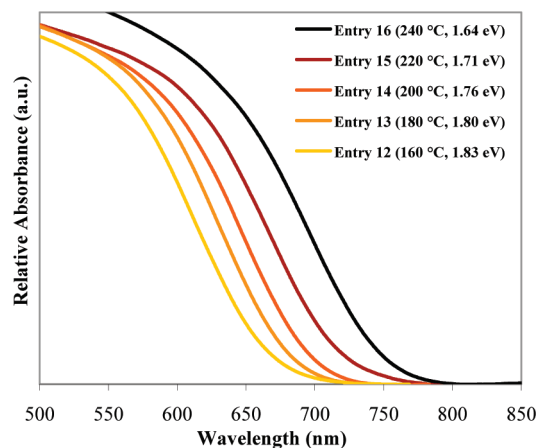


Figure 3. Normalized UV–vis absorption spectra of typical $\text{CuIn}_{0.5}\text{Ga}_{0.5}\text{S}_2$ nanoparticles prepared at 160–240 °C, respectively, with calculated bandgaps.

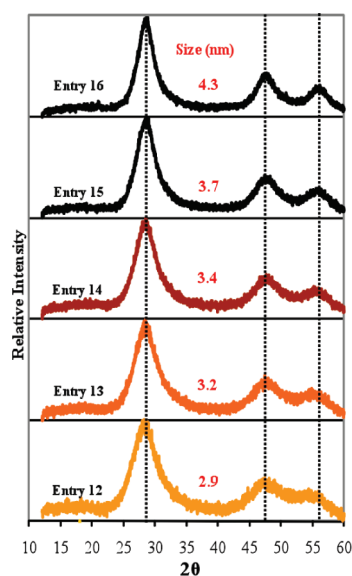


Figure 4. Normalized XRD data of typical $\text{CuIn}_{0.5}\text{Ga}_{0.5}\text{S}_2$ nanoparticles prepared at 160–240 °C, respectively, with calculated diameters.

The gradual sharpening of XRD peaks is indicative of the increasing particle sizes with increasing reaction temperatures (Figure 4). The particle sizes were determined to range from 2.9 to 4.3 nm. We observed the resulting bandgaps of $\text{CuIn}_{0.5}\text{Ga}_{0.5}\text{S}_2$ nanoparticles to be from 1.83 to 1.64 eV (Table 2, Figure 3).

A HRTEM image of $\text{CuIn}_{0.9}\text{Ga}_{0.1}\text{S}_2$ nanoparticles (Table 1, entry 2) is shown in Figure 5. Sizes of $\text{CuIn}_{0.5}\text{Ga}_{0.5}\text{S}_2$ nanoparticles range from 2.9 to 4.3 nm when synthesized at 160 to 240 °C, respectively, and the range is consistent with the HRTEM images (see the Supporting Information).

The selected area electron diffraction (SAED) pattern of $\text{CuIn}_{0.7}\text{Ga}_{0.3}\text{S}_2$ nanoparticles (Table 1, entry 4) supports a high crystallinity of chalcopyrite phase (Figure 6).

Potentially, these nanoparticles can be incorporated into next-generation quantum-dot-based solar cells. Therefore, the ability to prepare quaternary $\text{CuIn}_x\text{Ga}_{1-x}\text{S}_2$ ($0 \leq x \leq 1$)

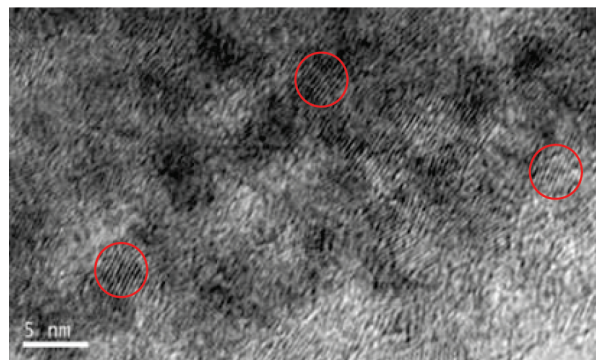


Figure 5. HRTEM image of $\text{CuIn}_{0.9}\text{Ga}_{0.1}\text{S}_2$ nanoparticles at 160 °C.

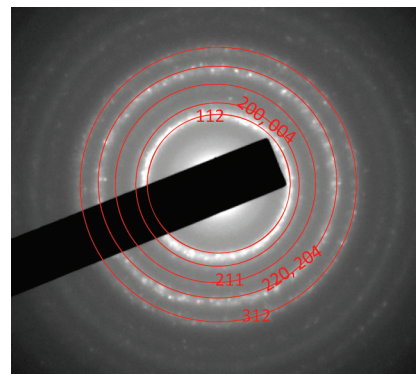


Figure 6. SAED pattern of $\text{CuIn}_{0.7}\text{Ga}_{0.3}\text{S}_2$ nanoparticles at 160 °C.

chalcopyrite nanoparticles with precise control of stoichiometry is important for controlling bandgaps. The reaction temperatures are also critical for fine control of nanoparticle sizes and bandgaps. We have shown that by exploiting the microwave assisted decomposition of two different SSPs in the presence of 1,2-ethanedithiol, we efficiently prepared $\text{CuIn}_x\text{Ga}_{1-x}\text{S}_2$ ($0 \leq x \leq 1$) nanoparticles. Short reaction times of less than 1 h have been achieved for the preparation of these nanoparticles. Two major advantages of our approach are precise stoichiometric control of In and Ga ratio and controlling the size of nanoparticles by reaction temperatures thus engineering bandgaps. A wide range of bandgaps can be engineered through a combination of precise control of elemental composition and particle sizes. We are currently exploring the use of various related SSPs to prepare multinary nanoparticles that exhibit an even wider range of bandgaps and other unique optoelectric behaviors.

Acknowledgment. The authors are thankful for financial support received through DOE EPSCoR Grant DE-FG02-04ER46142. A.T. and A.P. acknowledge financial support from NSF-MRI 0722699 (XPS) and 0521315 (TEM).

Supporting Information Available: Experimental procedures, additional UV–vis, XRD, ICP-OES, HRTEM images, and XPS data (PDF). This material is available free of charge via the Internet at <http://pubs.acs.org/>.